The Pharmacogenomics Journal (2002) 2, 377–382

www.nature.com/tpj

ORIGINAL ARTICLE

Differential expression of VAMP2/synaptobrevin-2 after antidepressant and electroconvulsive treatment in rat frontal cortex

M Yamada[1]
K Takahashi[1]
M Tsunoda[1]
G Nishioka[2]
K Kudo[2]
H Ohata[1]
K Kamijima[2]
T Higuchi[3]
K Momose[1]
M Yamada[2,4]

[1]*Department of Pharmacology, Showa University School of Pharmaceutical Sciences, Tokyo, Japan;* [2]*Department of Psychiatry, Showa University School of Medicine, Tokyo, Japan;* [3]*Kohnodai Hospital, National Center of Neurology and Psychiatry, Chiba, Japan;* [4]*Department of Psychiatry, Showa University Karasuyama Hospital, Tokyo, Japan*

Correspondence:
M Yamada, Department of Psychiatry, Showa University Karasuyama Hospital, 6-11-11 Kitakarasuyama, Setagaya, Tokyo 157-8577, Japan
Tel: +81 3 3300 5231
Fax: +81 3 3308 9710
E-mail: mitsu@med.showa-u.ac.jp

Received: 27 January 2002
Revised: 30 June 2002
Accepted: 7 July 2002

ABSTRACT
The biological basis for the therapeutic mechanisms of depression is still unknown. We have previously performed expressed-sequence tag (EST) analysis to identify some molecular machinery responsible for antidepressant effect. Then, we developed our original cDNA microarray, on which cDNA fragments identified as antidepressant-related genes/ESTs were spotted. In this study, with this microarray followed by Western blot analysis, we have demonstrated the induction of vesicle-associated membrane protein 2 (VAMP2/synaptobrevin-2) in rat frontal cortex not only after chronic antidepressant treatment, but also after repeated electroconvulsive treatment. On the other hand, expression of SNAP-25 and syntaxin-1 was not changed by these treatments. These components make a soluble *N*-ethylmaleimide-sensitive fusion protein attachment protein receptor complex with VAMP2 and mediate the synaptic vesicle docking/fusion machinery. In conclusion, it is suggested that VAMP2/synaptobrevin-2 plays important roles in the antidepressant effects. Our results may contribute to a novel model for the therapeutic mechanism of depression and new molecular targets for the development of therapeutic agents.
The Pharmacogenomics Journal (2002) **2**, 377–382. doi:10.1038/sj.tpj.6500135

Keywords: differential cloning; gene expression; depression; SSRI; microarray

INTRODUCTION

Depression is one of the major psychiatric diseases that is estimated to affect 12–17% of the population during the lifetime of an individual.[1] It has been demonstrated that typical antidepressants acutely inhibit the monoamine reuptake in nerve terminals resulting in significant increase in synaptic concentrations of monoamines, noradrenaline or serotonin. However, there is a latency period of several weeks before the onset of clinical effect of antidepressants. Repeated electroconvulsive treatment (ECT) is another therapy that is widely used, particularly in the treatment of drug-resistant depression. It is an efficient treatment modality, although the basis for its therapeutic mechanism is still unknown. The delay of clinical effect from the beginning of antidepressants and ECT could be the result of indirect regulation of neural signal transduction systems or changes at the molecular level by an action on gene transcription. Indeed, there are selective effects of antidepressants on specific immediate early genes and transcription factors including c-fos,[2,3] zif268,[2] NGFI-A[4,5] and the phosphorylation of CRE-binding protein.[6] It is also reported that ECT affects the expression of c-fos, junB and Narp.[7,8] These molecules activate or repress genes encoding specific proteins by binding to a regulating element of DNA. These functional proteins may be involved in critical steps in mediating treatment-induced neural plasticity.

We have recently performed expressed-sequence tag (EST) analysis to identify some common biological changes induced after chronic treatment of two different classes of antidepressants, imipramine (a tricyclic antidepressant) and sertraline (a serotonin-selective reuptake inhibitor (SSRI)). Identification of quantitative changes in gene expression that occur in the brain after chronic antidepressant treatment can yield novel molecular markers that would be useful in the diagnosis and treatment of depression. Until now, we have molecularly cloned cDNA fragments as ESTs, which were named after antidepressant-related gene-s(ADRG).[9] More recently, for high-throughput secondary screening of candidate genes, ADRG cDNAs were spotted on glass slides, and we developed our original cDNA microarray (ADRG microarray).[10,11] An important task for the future will be to ascertain which of these changes in gene expression are directly relevant to the therapeutic effects of antidepressants. In this study, we used ADRG microarray to search for some genes commonly induced after chronic antidepressant treatment and repeated ECT.

Here, we first reported that the expression of ADRG14, a vesicle-associated membrane protein 2 (VAMP2/synaptobrevin-2), is commonly increased in rat frontal cortex after chronic antidepressant treatment and repeated ECT. VAMP2 is a key component of the synaptic vesicle docking/fusion machinery that forms the soluble N-ethylmaleimide-sensitive fusion protein attachment protein receptor (SNARE) complex.[12–15]

RESULTS

Identification of ADRG14 as VAMP2

In the present study, we used an ADRG microarray for high-throughput, secondary screening to identify genes commonly affected by antidepressant and ECT. Figure 1 shows the pseudo-color image of the ADRG microarray after hybridization with samples obtained from sertraline- (a) or ECT-treated (b) rat frontal cortex. As expected, we obtained low background and consistent results in duplicated experiments. After normalization of the signals for both negative and positive controls, several spots of interest on the ADRG microarray showed increased or decreased fluorescence intensities after chronic sertraline treatment or repeated ECT. Interestingly, the fluorescence intensities of the spots for ADRG14 were increased 2.3 times in the sertraline group and 2.1 times in the ECT group, when compared to controls. These data were reproducible and interassay variation was negligible, when the differences of fluorescence intensities ($\pm$2-fold) were regarded as significant.

The size of ADRG14 fragment obtained from initial EST analysis was 224 bp. Sequence and homology analysis of ADRG14 with the EMBL/GeneBank database showed perfect matches to rat VAMP2 gene (NM012663[16]).

The induction of VAMP2 after chronic antidepressant treatment with two different classes of antidepressants, imipramine or sertraline, was also confirmed by RT-PCR analysis. The reproducible band corresponding to VAMP2 (784 bp) existed on a gel. As shown in Figure 2, we have demonstrated that the treatment with either imipramine or sertraline significantly induced the expression of VAMP2 mRNA levels (134.8$\pm$11.0% or 141.6$\pm$7.8%, $P<0.05$, ANOVA followed by the Dunnett's test, respectively) after normalization by GAPDH expression. The expression of VAMP2 was also significantly increased in repeated ECT-treated rat frontal cortex (159.2$\pm$10.4%, $P<0.05$, ANOVA followed by the Dunnett's test).

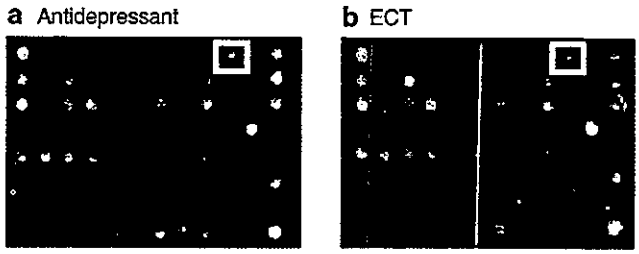

Figure 1 Image analysis of ADRG microarray after hybridization with fluorescence probes. Ninety-six spots representing ADRG1-96 are shown here. The pseudo-color image of control group data (green) and chronic sertraline treatment group (red) were overlapped (a). As expected, we obtained low background and consistent results in duplicated experiments. In addition, the pseudo-color image of control group data (green) and repeated ECT group (red) were also overlapped (b). The spot with blue rectangle represents ADRG14 (VAMP2/synaptobrevin-2). Interestingly, the fluorescence intensities of the spots were increased 2.3 times in the sertraline group and 2.1 times in the ECT group, when compared to controls.

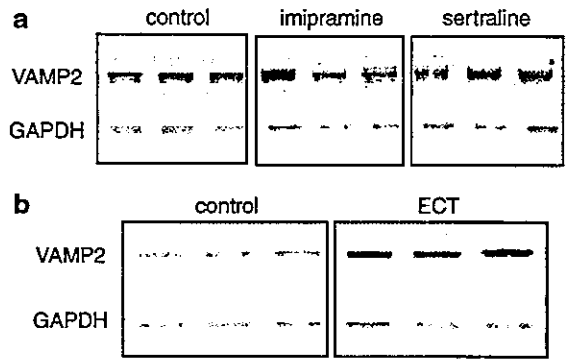

Figure 2 Induction of VAMP2 mRNA after chronic antidepressant treatment (a) and repeated ECT (b) revealed by RT-PCR. Total RNA was extracted from rat frontal cortex treated either with vehicle (control, lanes a1–3), 10 mg/kg of imipramine (lanes a4–6) or 10 mg/kg of sertraline (lanes a7–9) for 21 days, and used for RT-PCR analysis. Total RNA samples extracted from rat frontal cortex treated either with sham operation (control, lanes a1-3) or repeated ECT (lanes a4-6) were also used for RT-PCR analysis. The reproducible single band corresponding to VAMP2 at the size of 784 bp existed on a gel. This figure represents a typical result of three independent experiments. Treatment with imipramine or sertraline increased the expression of VAMP2 in rat frontal cortex when compared to control samples (a). In addition, repeated ECT also increased the expression of VAMP2 in rat frontal cortex when compared to control samples (b).

Western Blot Analysis using Anti-VAMP2 Antibody

Genes are transcribed to various mRNAs and then translated into proteins that may be post-translationally modified and subsequently function as the ultimate effecting molecules in the cell. To determine whether the increase of VAMP2 mRNA levels was associated with a change of protein content, we analyzed VAMP2 immunoreactivity in rat frontal cortex with Western blot analysis. As shown in Figure 3, the existence of a single band of approximately 18 kDa was confirmed. Treatment with imipramine or sertraline induced a significant increase in VAMP2 immunoreactivity (418.0±22.3% or 387.2±17.5%, respectively) when compared to control samples (Table 1). Interestingly, VAMP2 immunoreactivity was also significantly increased after repeated ECT (175.6±10.1%, Figure 3, Table 1). These observations indicate that changes of VAMP2 gene expression may contribute to the therapeutic efficacy of chronic antidepressant treatment or repeated ECT. On the other hand, a single administration of antidepressant or acute ECT did not affect VAMP2 immunoreactivity when compared to control samples (Figure 3).

We then investigated the expression of two other proteins of regulated secretory pathways, syntaxin-1 and SNAP-25, because they make a SNARE complex with VAMP2. Concomitantly, immunoreactivity for syntaxin and SNAP-25 was unaffected by chronic antidepressant treatment or repeated ECT (Figures 4 and 5). In addition, a single administration of antidepressant or acute ECT did not affect syntaxin and synaptosome-associated protein of 25 kDa (SNAP-25) immunoreactivity when compared to control samples (Figures 4 and 5).

Table 1 Induction of VAMP2 immunoreactivity after chronic antidepressant treatment with two different classes of antidepressants, imipramine or sertraline, and repeated ETC

Treatment	*VAMP2 expression*
Control	100.0±7.1
Imipramine	418.0±22.3*
Sertraline	387.2±17.5*
Control	100.0±4.1
Repeated ECT	175.6±10.1*

Data are expressed as % of the control data (mean±SEM) of three independent experiments.
*$P<0.05$, ANOVA followed by the Dunnett's test.

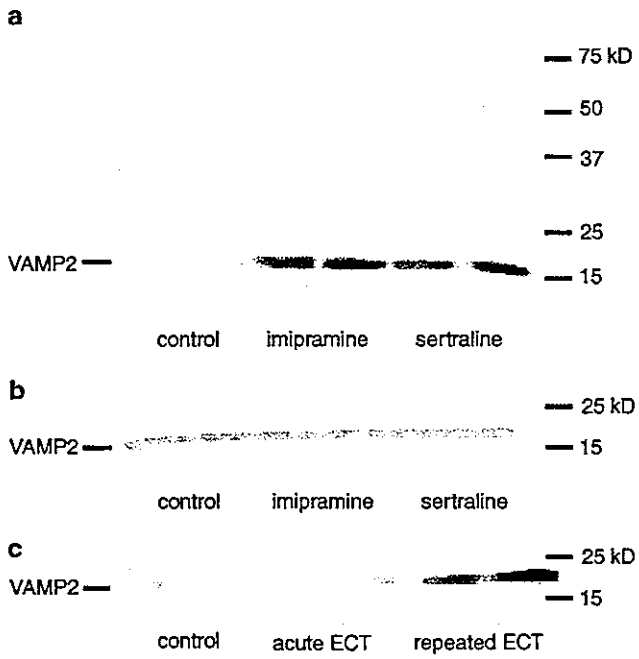

Figure 3 Western blot analysis of VAMP2 after chronic antidepressant treatment (a), a single antidepressant treatment (b) or ECT (c). Protein sample was prepared from rat frontal cortex treated either with vehicle (control, lanes 1–2), 10 mg/kg of imipramine (lanes 3–4) or sertraline (lanes 5–6) and used for Western blot analysis as described in Materials and methods. In addition, protein sample was also prepared from rat frontal cortex treated either with sham operation (control, lanes 1–2), acute ECT (lanes 3–4) or repeated ECT (lanes 5–6). This figure represents a typical result of three independent experiments.

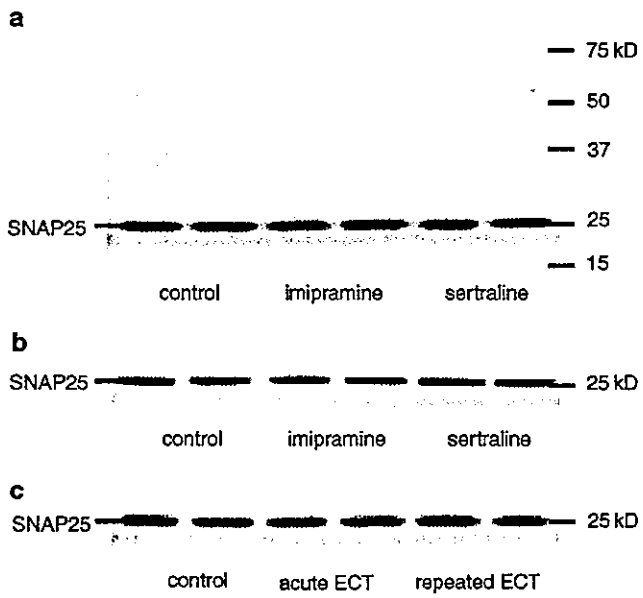

Figure 4 Western blot analysis of SNAP25 after chronic antidepressant treatment (a), a single antidepressant treatment (b) or ECT (c). Protein sample was prepared from rat frontal cortex treated either with vehicle (control, lanes 1–2), 10 mg/kg of imipramine (lanes 3–4) or sertraline (lanes 5–6) and used for Western blot analysis as described in Materials and methods. In addition, protein sample was also prepared from rat frontal cortex treated either with sham operation (control, lanes 1–2), acute ECT (lanes 3–4) or repeated ECT (lanes 5–6). This figure represents a typical result of three independent experiments.

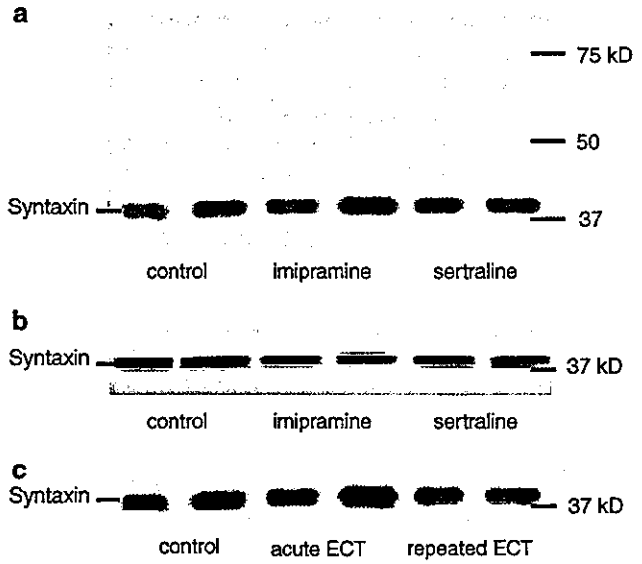

Figure 5 Western blot analysis of syntaxin after chronic antidepressant treatment (a), a single antidepressant treatment (b) or ECT (c). Protein sample was prepared from rat frontal cortex treated either with vehicle (control, lanes 1–2), 10 mg/kg of imipramine (lanes 3–4) or sertraline (lanes 5–6) and used for Western blot analysis as described in Materials and methods. In addition, protein sample was also prepared from rat frontal cortex treated either with sham operation (control, lanes 1–2), acute ECT (lanes 3–4) or repeated ECT (lanes 5–6). This figure represents a typical result of three independent experiments.

DISCUSSION

In the present study, we focused on an EST, ADRG14, whose expression was increased after chronic antidepressant treatment and repeated ECT. Sequence and homology analysis of ADRG14 using the EMBL/GeneBank database showed significant matches to rat VAMP2.[16] Considerable evidence indicates that VAMP2 is an important component of the regulated secretory pathway at nerve terminals. It has been reported that VAMP2 interacts with syntaxin-1 and SNAP-25, constituting the SNARE complex, the biochemical intermediate essential for vesicular transport and/or fusion processes.[12–15] Fusion of vesicles with the plasma membrane leads to exocytosis, which mediates the release of neurotransmitter into the synaptic cleft. In this context, pharmacological modulation of VAMP2 gene expression would also be predicted to alter the secretory response of neurons. In the present study, we demonstrated a significant increase of both VAMP2 mRNA and protein levels in rat frontal cortex after chronic treatment with two different classes of antidepressants, imipramine and sertraline. Our data suggest that VAMP2 may be one of the common functional molecules induced after chronic antidepressant treatment. This altered pattern of VAMP2 gene expression was also observed after repeated ECT.

On the other hand, single administration of antidepressant or acute ECT did not induce VAMP2 expression, suggesting that the induction of VAMP2 is due to the long-term therapeutic action of these treatments. These findings suggest that genome-dependent alterations of the secretory behavior of neurons may be an important component of the therapeutic action of antidepressants and ECT. Interestingly, the work of others has shown that acute and chronic administration of antidepressants diminishes the release of glutamate and aspartate, and inhibits veratridine-evoked 5-HT release.[17]

An important feature of the action of antidepressants and ECT is that they did not globally alter the expression of other membrane-trafficking proteins. In contrast to the enhanced expression of VAMP2, we detected no significant change in the expression of other synaptic vesicle proteins, syntaxin-1 and SNAP-25. Although there are more than a dozen synaptic vesicle proteins,[18] we chose to investigate the expression of syntaxin-1 and SNAP-25 because they make a SNARE complex with VAMP2 and mediate the synaptic vesicle docking/fusion machinery. We reasoned that a coordinated change of VAMP2 and the expression of syntaxin-1 and SNAP-25 might signal a change in the overall number of SNARE complexes. An antidepressant-induced change in the expression of syntaxin-1 and SNAP-25, associated predominantly with the presynaptic plasma membrane, would have been indicative of more complex changes in the secretory pathway, such as an increase in the number of active zones. Instead, the absence of such a coordinated change in syntaxin-1 and SNAP-25 expression indicates that antidepressants or ECT produces a more selective modification of the regulated secretory machinery. Additional work will be necessary to understand the role of selective VAMP2 induction in rat frontal cortex.

Previously, we have demonstrated that a unique cysteine-rich protein, cysteine string protein (CSP), is clearly increased in the rat brain after chronic antidepressant treatment.[11] There are several reports indicating that the function of CSP in the central nervous system is to modulate the activity of presynaptic calcium channels, resulting in neurotransmitter release at the nerve terminal.[19,20] Similar to VAMP2, CSP is also localized to synaptic vesicle membranes and interacts with VAMP2 in rat brain.[21,22] Taken together, this coordinated induction of two presynaptic molecules may suggest that the number of secretory organelles, which includes both small clear vesicles as well as large dense-core granules, might be increased after chronic antidepressant treatment and repeated ECT. Interestingly, it is previously reported that the expression of VAMP2 and CSP was also enhanced by lithium ions, a well-established pharmacotherapy for the treatment of recurrent manic-depressive illness, in differentiated PC12 cells.[23,24] The coordinated induction of these genes may contribute to the therapeutic efficacy in mood disorders not only for depression, but also for manic-depressive illness.

Our findings suggest that gene-expression dependent alterations of the secretory behavior of neurons may be an important component of the pharmacological action of antidepressants and ECT. Thus, it will be of interest to determine whether these changes in the frontal cortex

contribute to clinical effects in patients treated with antidepressants and ECT. Indeed, the frontal cortex is one of the several brain regions that would be involved in the endocrine, emotional, cognitive, and vegetative abnormalities found in depressed patients. In the frontal cortex, glucose metabolism, blood flow, and electroencephalograph activity are altered in depressed patients.[25] It is reasonable to understand that alterations of mood, neurovegetative signs, or even social behavior of depressed patients reflect some changes in patterns of synaptic activity in the brain. Additional work would be necessary to test this hypothesis.

In conclusion, the current investigation has identified VAMP2 as a novel molecular target for antidepressants and ECT. Our findings offer novel insights into the actions of antidepressants and ECT that may be of both basic and clinical significance. Furthermore, the ADRG microarray we developed seemed to be a powerful tool for the discovery of novel therapeutic targets for future drug development with a new class of action in the brain.

MATERIALS AND METHODS

Experimental animals

Male Sprague-Dawley rats (age 7–10 weeks, Sankyo Labo Service Co. , Tokyo, Japan) were housed in a temperature-controlled environment with a 12 h light/12 h dark cycle and free access to food and water. Rats were randomly separated into control and treated groups. Six rats were used for each treatment group. Experimental animals for chronic treatment of antidepressants received either vehicle for 21 days, 10 mg/kg of imipramine (Sigma Chemical, MO, USA), or sertraline (Pfizer Pharmaceuticals Inc., NY, USA), dissolved in 1.5% Tween 80, by daily intraperitoneal injection. Rats for ECT were anesthetized with sevoflurane and received a 90 mA, 1.0 sec electric shock via ear-clip electrodes once (acute ECT group), or every other day for 14 days (repeated ECT group). ECT employed the Ugo Basile Model 7801 Unipolar square-wave electroconvulsive stimulation pulse generator (Stoelting Co., IL, USA). The control group was treated exactly the same as ECT-treated rats, but without the administration of the electric current. Animals were killed by decapitation 24 h after the final antidepressant administration or ECT treatment, and the brain was quickly removed, dissected and then frozen in liquid nitrogen immediately and stored at –80°C until use. All studies using animals were carried out in accordance with animal protocols approved by the National Institutes of Health, OPRR Public Health Service Policy on Humane Care and Use of Laboratory Animals.

Identification of ADRG14

Fabrication of the ADRG microarray and fluorescence image analysis was done as described by our group previously.[10] Briefly, each of the cDNA inserts for ADRG were amplified by vector primers and negative controls, and 10 different kinds of housekeeping genes were spotted in duplicate on glass slides using a GMS417 Arrayer (Affymetrix, Inc., CA, USA). To make the fluorescence-labeled probe for hybridization, poly A^+ RNA was purified from total RNA that was pooled with three independent control or treated groups. One microgram of poly A^+ RNA from control or treated samples was converted to cDNA in the presence of Cy-5- or Cy-3-dUTP, respectively, to make fluorescence-labeled probes. Hybridization of probes to the microarray was done competitively in duplicate. The probes were mixed and placed on an array, overlaid with a coverslip, and hybridized for 16.5 h at 65°C. After the hybridization and washing procedure, each slide was scanned with a GMS418 Array Scanner (Affymetrix, Inc., CA, USA). Gene expression levels were quantified and analyzed using ImaGene software (Bio-Discovery Ltd. Swansea, UK). With our preliminary experiment (data not shown), the differences of fluorescence intensities (±2-fold) were regarded as significant.

Sequence analysis of ADRG14 was performed by dideoxy sequencing methods. Homology search and sequence alignment was done using the FASTA search servers at the National Center for Biotechnology Information.

Messenger RNA Expression Analysis with RT-PCR

The first strand of cDNA was synthesized with reverse transcriptase and 1 μM of oligo-dT primer from 2 μg of total RNA samples treated with RNase-free DNase I and diluted to a final volume of 100 μL. One microliter of each cDNA sample was added to 24 μl of PCR reaction mixture containing 0.5 μM of a pair of primers for VAMP2 (5′-AGTCTAGTTTGCTTCCCTTACC-3′ and 5′-CAGTTTA-CATCTCCTTGGTTCC-3′) (Amersham Pharmacia Biotech, Tokyo, Japan). A pair of primers for a housekeeping gene, glyceraldehyde-3-phosphate-dehydrogenase (GAPDH, 5′-TGAAGGTCGGTGTCAACGGATTTGGC-3′ and 5′-CATG-TAGGCCATGAGGTCCACCAC-3′) was also used for normalization. To ensure the fidelity of this analysis, we assayed several cycles of PCR to determine the linear range for the amplification of the PCR product. Amplification of VAMP2 was performed as follows: 3 min at 94°C for initial denaturation, 22 cycles of 94°C denaturing for 30 s, 51°C annealing for 30 s, and 72°C extension for 1 min, followed by a final extension at 72°C for 7 min. Amplification of GAPDH was performed as follows: 3 min at 94°C for initial denaturation, 18 cycles of 94°C denaturing for 30 s, 51°C annealing for 30 s, and 72°C extension for 1 min, followed by a final extension at 72°C for 7 min. The PCR products were electrophoresed in a 1% agarose gel containing SYBR green, a nucleic acid gel stain reagent (Takara, Tokyo, Japan). The optical density of the digitized image was quantified using a fluorescence image analyzer, FM-bio II (Hitachi, Tokyo, Japan). Without reverse transcriptase, we found no PCR products in a gel, indicating that genomic DNA contamination was negligible.

Western Blot Analysis

Frontal cortex from control and treated rats was homogenized in ice-cold Sucrose-Tris buffer (250 mM sucrose, 50 mM Tris-HCl, 5 mM EDTA, 10 mM EGTA, 0.3%. mercaptoethanol, pH 7.4). The protein concentration was deter-

mined by the Bradford method using the Bio-Rad protein assay kit. Each fraction (20 μg of protein) was separated by 10% SDS-PAGE after solubilization and boiling in Laemmli buffer. Electrophoretic protein was transferred from gels to nitrocellulose membranes using standard techniques. The membranes were blocked and incubated with antibody using Aurora Western Blotting kit (ICN Biomedicals Inc., CA, USA) following the manufacturer's instructions. The primary antibodies for VAMP2, SNAP-25 or syntaxin-1 (Wako, Osaka, Japan) were diluted 1:500, 1:1000, or 1:500, respectively, in blocking buffer followed by appropriate secondary antibodies. The immunoreactive bands were visualized on film by the ECL system. To ensure the fidelity of this analysis, we assayed the film exposed only in the linear range. The optical density of the digitized image was quantified using NIH image, software running on an Apple Computer. NIH Image is a public domain program (developed at the US National Institutes of Health) and available on the Internet at http://rsb.info.nih.gov/nih-image/).

Statistical analysis

Data are given as mean±SEM for the group. Differences were assessed using Analysis of Variance (ANOVA) followed by the Dunnett's test. A value of $P<0.05$ was regarded as significant.

ACKNOWLEDGEMENTS

Sertraline was kindly supplied by Pfizer Pharmaceuticals Inc., NY, USA. M Yamada was supported by a fellowship from the Japan Foundation for Aging and Health. M Tsunoda was supported by a fellowship from the Japan Health Sciences Foundation. This work was in part supported by Health Science Research Grants from Ministry of Health, Labour and Welfare, Ministry of Education, Culture, Sport, Science, and Technology, and Japan Society for the Promotion of Science

DUALITY OF INTEREST

None declared.

REFERENCES

1 Wittchen HU, Knauper B, Kessler RC. Lifetime risk of depression. *Br J Psychiatry* 1994; s26: 16–22.
2 Dahmen N, Fehr C, Reuss S, Hiemke C. Stimulation of immediate early gene expression by desipramine in rat brain. *Biol Psychiatry* 1997; **42**: 317–323.
3 Torres G, Horowitz JM, Laflamme N, Rivest S. Fluoxetine induces the transcription of genes encoding c-fos, corticotropin-releasing factor and its type 1 receptor in rat brain. *Neuroscience* 1998; **87**: 463–477.
4 Johansson IM, Bjartmar L, Marcusson J, Ross SB, Seckl JR, Olsson T. Chronic amitriptyline treatment induces hippocampal NGFI-A glucocorticoid receptor and mineralocorticoid receptor mRNA expression in rats. *Brain Res Mol Brain Res* 1998; **62**: 92–95.
5 Bjartmar L, Johansson IM, Marcusson J, Ross SB, Seckl JR, Olsson T. Selective effects on NGFI-A, MR, GR and NGFI-B hippocampal mRNA expression after chronic treatment with different subclasses of antidepressants in the rat. *Psychopharmacology* 2000; **151**: 7–12.
6 Thome J, Sakai N, Shin K, Steffen C, Zhang YJ, Impey S *et al*. cAMP response element-mediated gene transcription is upregulated by chronic antidepressant treatment. *J Neurosci* 2000; **20**: 4030–4036.
7 Chen J, Nye HE, Kelz MB, Hiroi N, Nakabeppu Y, Hope BT *et al*. Regulation of delta FosB and FosB-like proteins by electroconvulsive seizure and cocaine treatments. *Mol Pharmacol* 1995; **48**: 880–889.
8 Reti IM, Baraban JM. Sustained increase in Narp protein expression following repeated electroconvulsive seizure. *Neuropsychopharmacology* 2000; **23**: 439–443.
9 Yamada M, Kiuchi Y, Nara K, Kanda Y, Morinobu S, Momose K *et al*. Identification of a novel splice variant of heat shock cognate protein 70 after chronic antidepressant treatment in rat frontal cortex. *Biochem Biophys Res Commun* 1999; **261**: 541–545.
10 Yamada M, Yamada M, Yamazaki S, Takahashi K, Nishioka G, Kudo K *et al*. Identification of a novel gene with RING-H2 finger motif induced after chronic antidepressant treatment in rat brain. *Biochem Biophys Res Commun* 2000; **278**: 150–157.
11 Yamada M, Yamada M, Yamazaki S, Takahashi K, Nara K, Ozawa H *et al*. Induction of cysteine string protein after chronic antidepressant treatment in rat frontal cortex. *Neurosci Lett* 2001; **301**: 183–186.
12 Trimble WS, Cowan DM, Scheller RH. VAMP-1: a synaptic vesicle-associated integral membrane protein. *Proc Natl Acad Sci USA* 1988; **85**: 4538–4542.
13 Oyler GA, Higgins GA, Hart RA, Battenberg E, Billingsley M, Bloom FE *et al*. The identification of a novel synaptosomal-associated protein, SNAP-25, differentially expressed by neuronal subpopulations. *J Cell Biol* 1989; **109**: 3039–3052.
14 Bennett MK, Calakos N, Scheller RH. Syntaxin: a synaptic protein implicated in docking of synaptic vesicles at presynaptic active zones. *Science* 1992; **257**: 255–259.
15 Weis WI, Scheller RH. Membrane fusion. SNARE the rod, coil the complex. *Nature* 1998; **395**: 328–329.
16 Elferink LA, Trimble WS, Scheller RH. Two vesicle-associated membrane protein genes are differentially expressed in the rat central nervous system. *J Biol Chem* 1989; **264**: 11 061–11 064.
17 Golembiowska K, Dziubina A. Effect of acute and chronic administration of citalopram on glutamate and aspartate release in the rat prefrontal cortex. *Pol J Pharmacol* 2000; **52**: 441–448.
18 Sudhof TC. The synaptic vesicle cycle: a cascade of protein-protein interactions. *Nature* 1995; **375**: 645–653.
19 Gundersen CB, Umbach JA. Suppression cloning of the cDNA for a candidate subunit of a presynaptic calcium channel. *Neuron* 1992; **9**: 527–537.
20 Umbach JA, Zinsmaier KE, Eberle KK, Buchner E, Benzer S, Gundersen CB. Presynaptic dysfunction in Drosophila csp mutants. *Neuron* 1994; **13**: 899–907.
21 Leveque C, Pupier S, Marqueze B, Geslin L, Kataoka M, Takahashi M *et al*. Interaction of cysteine string proteins with the alpha1A subunit of the P/Q-type calcium channel. *J Biol Chem* 1998; **273**: 13 488–13 492.
22 Chamberlain LH, Burgoyne RD. Cysteine-string protein: the chaperone at the synapse. *J Neurochem* 2000; **74**: 1781–1789.
23 Cordeiro ML, Umbach JA, Gundersen CB. Lithium ions enhance cysteine string protein gene expression in vivo and in vitro. *J Neurochem* 2000; **74**: 2365–2372.
24 Cordeiro ML, Umbach JA, Gundersen CB. Lithium ions Up-regulate mRNAs encoding dense-core vesicle proteins in nerve growth factor-differentiated PC12 cells. *J Neurochem* 2000; **75**: 2622–2625.
25 Drevets W, Videen T, Price J, Preskorn S, Carmichael S, Raichle M. A functional anatomical study of unipolar depression. *J Neurosci* 1992; **12**: 3628–3641.

Brief Report

Deactivation by Benzodiazepine of the Basal Forebrain and Amygdala in Normal Humans During Sleep: A Placebo-Controlled [^{15}O]H_2O PET Study

Naofumi Kajimura, M.D., Ph.D.
Masami Nishikawa, M.D., Ph.D.
Makoto Uchiyama, M.D., Ph.D.
Masaaki Kato, M.D., Ph.D.
Tsuyoshi Watanabe, M.D.
Toru Nakajima, M.D., Ph.D.
Toru Hori, M.D.
Tetsuo Nakabayashi, M.D., Ph.D.
Masanori Sekimoto, M.D., Ph.D.
Kenichi Ogawa, M.D.
Harumasa Takano, M.D., Ph.D.
Etsuko Imabayashi, M.D.
Masahiko Hiroki, M.D.
Takashi Onishi, M.D., Ph.D.
Takeshi Uema, M.D., Ph.D.
Yutaka Takayama, M.D.
Hiroshi Matsuda, M.D., Ph.D.
Masako Okawa, M.D., Ph.D.
Kiyohisa Takahashi, M.D., Ph.D.

Objective: The authors' goal was to identify differences in regional brain activity between physiological and benzodiazepine-induced sleep to clarify the brain structures involved in the drug's hypnotic effect.

Method: Using positron emission tomography, they compared regional cerebral blood flow during non-REM sleep in nine volunteers treated with placebo or triazolam, a short-acting benzodiazepine, in a double-blind, crossover design.

Results: Blood flow in the basal forebrain and amygdaloid complexes was lower during non-REM sleep when subjects were given triazolam than when they were given placebo.

Conclusions: The hypnotic effect of the benzodiazepines may be mediated mainly by deactivation of the forebrain control system for wakefulness and also by the anxiolytic effect induced by deactivation of the emotional center.

(Am J Psychiatry 2004; 161:748–751)

Benzodiazepine hypnotics, which have been used widely since the early 1960s, are known to act by agonistic modulation of γ-aminobutyric acid A ($GABA_A$) receptor subtypes. However, the pharmacological actions mediated by the $GABA_A$ receptor subtypes are still a matter of dispute (1). Therefore, many questions regarding the specific drug actions of the benzodiazepine hypnotics remain to be answered, including the question of which neuroanatomical sites are affected by these drugs.

Positron emission tomography (PET) has been used effectively to visualize the functional neuroanatomy of human sleep, and oxygen-15 water ([^{15}O]H_2O) PET, which is well suited to the investigation of sleep states of relatively short duration, has revealed changes in regional cerebral blood flow (rCBF) associated with human non-REM and REM sleep (2). The effects on human sleep of hypnotics acting on the $GABA_A$ receptor, including the newly developed nonbenzodiazepines, have also been explored by using PET (3). Unfortunately, previous studies failed to detect specific neuroanatomical sites for the actions of these hypnotics during sleep, possibly because of methodological problems. Therefore, we conducted a double-blind, crossover study of [^{15}O]H_2O PET with statistical parametric mapping to compare rCBF during human non-REM sleep after administration of triazolam or placebo.

Method

Fifteen healthy, right-handed, male university students (mean age=21.3 years, SD=1.0, range=20–23) served as study subjects. All gave written informed consent before participating in the study, which was approved by the Intramural Research Board of the National Center of Neurology and Psychiatry.

A maximum of eight intravenous injections of [^{15}O]H_2O were given to each subject during periods of wakefulness and light and deep non-REM sleep under continuous polygraphic monitoring on each experimental night of triazolam or placebo administration. The experiments were separated by a 1-week interval and did not include sleep deprivation. On the night of the experiment, electrodes were attached for polygraphy, and each subject lay face up on a scanner couch, with the head stabilized by an individually molded thermoplastic face mask secured to a plastic headholder. The headholder was fixed on the end of the scanner couch so that the head was protruding fully into the scanner field of view; the head was angled so that each subject's canthomeatal line was parallel to axial planes of the PET scanner.

After two PET scans for wakefulness were obtained in the eye-closed condition, the subject took a capsule containing either 0.25 mg triazolam or placebo at 10:00 p.m. The lights were turned out at 10:30 p.m., and three scans for light non-REM sleep (stage 2 sleep) and three for deep non-REM sleep (stages 3 and 4 sleep, slow wave sleep) were performed between 11:00 p.m. and 2:00 a.m., when the polygrams showed typical patterns for these sleep stages.

EEGs were recorded from disc electrodes placed at F3, F4, C3, C4, Fz, and Cz; A1 plus A2 were used for reference. Monopolar electro-oculograms were recorded from both canthi, and bipolar

electromyograms were recorded from the chin. Details of the polygraphic methodology are the same as in our previous study (4). Sleep stage scoring was carried out according to the standardized sleep manual of Rechtschaffen and Kales (5). Final evaluation of sleep stage scoring for each 90-second period during PET scanning was confirmed later by using C3 recording.

PET data were acquired with the use of a Siemens ECAT EXACT HR 961 scanner in the three-dimensional mode. The camera, having an axial field of view of 150 mm, acquired data simultaneously from 47 consecutive axial planes, which cover the whole brain, including the cerebrum, cerebellum, and brainstem. A spatial resolution of 3.8×3.8×4.7 mm of full width at half maximum was obtained after back-projection and filtering. The reconstructed image was displayed on a 128×128×47-voxel matrix (voxel size=1.732×1.732×3.125 mm). Transmission scanning was carried out before acquisition of the emission data by using a retractable, rotating $^{68}Ga/^{68}Ge$ source with three rods.

For each PET scan, an intravenous bolus of 7-mCi $[^{15}O]H_2O$ was automatically flushed over 15 seconds. Scanning was begun manually 1 second after the initial rise in head counts and was continued for 90 seconds. Arterial blood was sampled automatically throughout the scanning period with a flow-through radioactivity detector. Absolute CBF was quantified by using the autoradiographic technique (6, 7). Details of the PET data analysis are the same as in our previous study (8).

After the appropriate design matrix was specified, estimates of the subject and condition were determined according to a general linear model at each and every voxel. Parameter estimates were compared by using linear contrasts. The contrast of interest in this article was the main effect of the drug during non-REM sleep. These analyses generated statistical parametric maps that were subsequently transformed to the unit normal distribution. The exact level of significance of volumes of difference between conditions was characterized by peak amplitude. Clusters of voxels that had a peak z score greater than 3.09 (threshold $p<0.001$) were considered to show significant difference. A corrected p value of 0.05 was used as a statistical cluster threshold.

Results

We analyzed the PET data of nine of the 15 subjects, who provided us with complete sets of data during periods of wakefulness and light and deep non-REM sleep on the nights of triazolam and placebo administration. One-way analysis of variance showed no significant difference in the absolute values for global CBF during light or deep non-REM sleep between the placebo and triazolam conditions. Mean absolute global CBF during light non-REM sleep with placebo was 30.4 ml/100 g per minute (SD=5.1), and that with triazolam was 28.8 ml/100 g per minute (SD=4.6) ($F=0.51$, $p=0.49$). Mean absolute global CBF during deep non-REM sleep with placebo was 30.6 ml/100 g per minute (SD=3.2), and that with triazolam was 29.4 ml/100 g per minute (SD=3.1) ($F=0.64$, $p=0.44$).

When there are no differences in the absolute values for global CBF, comparison of normalized values for regional CBF is often more sensitive for detection of differences than comparison of absolute values and reflects real changes in rCBF (2, 8). Therefore, normalized rCBF values obtained for non-REM sleep with placebo were compared with those obtained with triazolam by analysis of covariance for the nine subjects who provided complete sets of data.

TABLE 1. Brain Regions Showing Significantly Lower Blood Flow in Nine Normal Volunteers During Non-REM Sleep After Triazolam Administration Than After Placebo Administration

Region	Brodmann's Area	Coordinates[a] x	y	z	z Score
Amygdaloid complex					
Left		−32	0	−18	4.68
Right		28	−4	−22	3.47
Caudal orbital basal forebrain					
Left		−18	20	−14	4.40
Right		22	10	−18	6.11
Basal forebrain					
Left		−14	0	−10	4.08
Right		10	0	−4	5.86
Anterior cingulate gyrus					
Left	24	−6	−4	36	3.68
Right	32	4	40	6	3.72
Posterior cingulate gyrus					
Left	23	−4	−16	28	3.33
Right	23	4	−26	26	3.65
Left insula	13	−40	−10	−4	3.29
Left prefrontal cortex superior frontal gyrus	10	−20	60	−8	4.62
Left precentral gyrus	44	−44	18	8	4.39
Left superior temporal gyrus	38	−50	20	−14	4.92
	22	−48	−14	8	4.02
Left superior parietal gyrus	7	−36	−66	48	3.75

[a] Coordinates are defined in the stereotactic space of Talairach and Tournoux (9), relative to the anterior commissure: x is the lateral distance from the midline (positive=right), y is the anteroposterior distance from the anterior commissure (positive=anterior), and z is the rostrocaudal distance from the bicommissural plane (positive=rostral). Significance level is employed at a height threshold of $p=0.001$, by reference to unit normal distribution ($z=3.09$), and at a threshold of corrected $p<0.05$.

Blood flow was lower in the basal forebrain, amygdaloid complexes, anterior (Brodmann's area 32, 24) and posterior (Brodmann's area 23) cingulate gyri, and the left neocortical regions, including the superior temporal gyrus (Brodmann's area 38, 22), precentral gyrus (Brodmann's area 44), superior frontal gyrus (prefrontal cortex) (Brodmann's area 10), superior parietal gyrus (Brodmann's area 7), and insula (Brodmann's area 13), during non-REM sleep when triazolam was given than when placebo was given (Table 1 and Figure 1). There was no significant increase in rCBF of any region during non-REM sleep under triazolam administration in comparison to that under placebo administration.

Discussion

Using functional neuroanatomical PET, we found that the basal forebrain and the amygdaloid complexes of human subjects showed deactivation during non-REM sleep after triazolam treatment. Wakefulness is known to be maintained by multiple neuronal populations spread out from the metencephalon to the diencephalon, the mesencephalic reticular formation, posterior and posterolateral hypothalamus, and basal forebrain cycle (10). Our data show that triazolam has its main impact on the basal fore-

FIGURE 1. Surface Projections and a Transverse Section of Brain Regions Showing Significantly Lower Levels of Blood Flow in Nine Normal Volunteers During Non-REM Sleep After Triazolam Administration Than After Placebo Administration

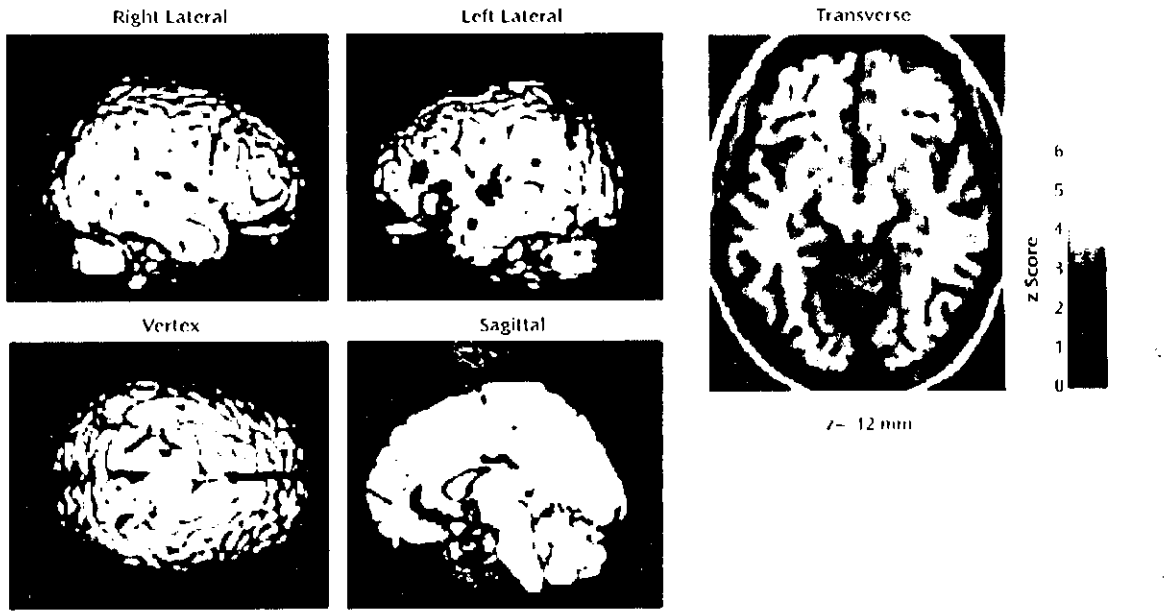

brain rather than on the other wake-promoting structures. Therefore, the hypnotic effect of the benzodiazepines may result mainly from inhibition of the forebrain control system for wakefulness. This is supported by the finding in our previous study (8) that the basal forebrain is deactivated during deep non-REM sleep in normal humans, suggesting that deactivation of the basal forebrain is involved in the non-REM sleep networks. Additionally, our present finding that triazolam deactivated the amygdaloid complexes, which are involved in emotional response, including anxiety and fear, during non-REM sleep, suggests that the anxiolytic effect of the benzodiazepines is also associated with their hypnotic effect.

Most benzodiazepines, including triazolam, induce particular changes in EEG activity and sleep stages. They decrease sleep latency and night awakenings, but, in terms of sleep architecture, they reduce slow wave sleep and REM sleep. Thus, the benzodiazepines have been mysterious agents with a paradoxical effect, and the mechanism explaining this effect has remained unclear. The present finding that triazolam deactivates the basal forebrain may account for the paradoxical effect. The basal forebrain is structurally and functionally heterogeneous. Since the basal forebrain contains the type of tonic neurons that are active specifically in wakefulness and the type that are active specifically in sleep (10), and since the latter type of neurons are particularly related to the induction of slow wave sleep (11), relatively diffuse deactivation of this region might facilitate initiation of sleep but inhibit slow wave sleep.

The left neocortical regions, including the superior temporal gyrus, precentral gyrus, superior frontal gyrus (prefrontal cortex), and superior parietal gyrus, were deactivated after triazolam administration. Asymmetric changes in rCBF during the sedative state induced by midazolam, a short-acting benzodiazepine, have been reported (12): midazolam was shown to decrease rCBF in the left prefrontal cortex in a dose-dependent fashion. The deactivation of the left neocortical regions by triazolam in the present study is basically consistent with the finding of the midazolam study, suggesting that left-hand cortical areas are more sensitive to the modulation of benzodiazepines.

Received Feb. 25, 2003; revision received Sept. 2, 2003; accepted Sept. 5, 2003. From the National Center Hospital for Mental, Nervous and Muscular Disorders. Address reprint requests to Dr. Kajimura, Musashi Clinic for Mental and Sleep Disorders, SF Bldg. 2F, 1-7-17 Misono-cho, Kodaira, Tokyo 187-0041, Japan; kajimura@sa2.so-net.ne.jp (e-mail).

Supported by a grant from the Ministry of Health, Labor and Welfare of Japan.

The authors thank Dr. Pierre Maquet for his critical comments and suggestions.

References

1. Müller WE: Pharmacology of the GABAergic/benzodiazepine system, in Pharmacology of Sleep. Edited by Kales A. Berlin, Springer-Verlag, 1995, pp 211–242
2. Maquet P: Functional neuroimaging of normal human sleep by positron emission tomography. J Sleep Res 2000; 9:207–231
3. Finelli LA, Landolt HP, Buck A, Roth C, Berthold T, Borbely AA, Achermann P: Functional neuroanatomy of human sleep

states after zolpidem and placebo: a $H_2{}^{15}O$-PET study. J Sleep Res 2000; 9:161–173
4. Kajimura N, Kato M, Okuma T, Sekimoto M, Watanabe T, Takahashi K: A quantitative sleep EEG study on the effects of benzodiazepine and zopiclone in schizophrenic patients. Schizophr Res 1995; 15:303–312
5. Rechtschaffen A, Kales A (eds): A Manual of Standardized Terminology, Techniques and Scoring System for Sleep Stages of Human Subjects: NIH Publication 204. Bethesda, Md, Public Health Service, National Institutes of Health, 1968
6. Herscovitch P, Markham J, Raichle ME: Brain blood flow measured with intravenous $H_2{}^{15}O$, I: theory and error analysis. J Nucl Med 1983; 24:782–789
7. Raichle ME, Martin WRW, Herscovitch P, Mintum MA, Makkam J: Brain blood flow measured with intravenous $H_2{}^{15}O$, II: implementation and validation. J Nucl Med 1983; 24:790–798
8. Kajimura N, Uchiyama M, Takayama Y, Uchida S, Uema T, Kato M, Sekimoto M, Watanabe T, Nakajima T, Horikoshi S, Ogawa K, Nishikawa M, Hiroki M, Kudo Y, Matsuda H, Okawa M, Takahashi K: Activity of midbrain reticular formation and neocortex during the progression of human non-rapid eye movement sleep. J Neurosci 1999; 19:10065–10073
9. Talairach J, Tournoux P: Co-Planar Stereotaxic Atlas of the Human Brain: Three-Dimensional Proportional System. Stuttgart, Germany, Georg Thieme, 1988
10. Sakai F, Mansari M, Jin JS, Zhang JG, Vanni-Mercier G: Posterior hypothalamus in the regulation of wakefulness and paradoxical sleep, in The Diencephalon and Sleep. Edited by Mancia M, Marini G. New York, Raven Press, 1990, pp 171–198
11. Koyama Y, Hayaishi O: Firing of neurons in the preoptic/anterior hypothalamic areas in rat: its possible involvement in slow wave sleep and paradoxical sleep. Neurosci Res 1994; 19:31–38
12. Veselis RA, Reinsel RA, Beattie BJ, Mawlawi OR, Feshchenko VA, DiResta GR, Larson SM, Blasberg RG: Midazolam changes cerebral blood flow in discrete brain regions: an $H_2{}^{15}O$ positron emission tomography study. Anesthesiology 1997; 87:1106–1117